Electronic supplementary information

Doppler splitting and expansion dynamics of laser-produced plasma plume under a high vacuum ambience†

Akira Kuwahara,*[a] Kenta Murakami,[a] Hideki Tomita,[a] Kayo Sawada,[b] Youichi Enokida[a]

[a]Department of Applied Energy, Graduate School of Engineering, Nagoya University, Aichi 464-8603, Japan

[b]Institute of Materials and Systems for Sustainability, Nagoya University, Aichi 464-8601, Japan

* Corresponding author: Akira Kuwahara

Furo-cho, Chikusa-ku, Nagoya, Aichi 464-8603, Japan.

Phone No: +81 52 789 5936

E-mail: akuwahara@energy.nagoya-u.ac.jp

Laser ablation threshold evaluation

The threshold pulse energy for laser ablation was evaluated by varying the pulse energy using ND filters (NDK01, Thorlabs). The relationship between the transmittance and the pulse energy is shown in Fig. S1. The threshold pulse energy was evaluated to be approximately 0.5 mJ from the extrapolation of the linear region.

Formation of a crater and its influence on transmittance

Since laser ablation ejects the surface material at intense laser pulses, it causes crater formation and changes the transmittance, which is called the crater effect. In this study, the accumulation of laser shots was required to restructure the absorption profile with a slow wavelength scan ($\approx$ 1 Hz). The relationship between the transmittance and the number of laser shots is shown in Fig. S2.

Size of a crater generated by laser ablation

The typical digital image of the ablated crater was observed using a microscope (Eclipse Ci POL, Nikon) and is shown in Fig. S3. The distance on the major axis was approximately 220 μm. The heat-affected zone (HAZ) depends on the pulse width. The HAZ of nanosecond laser ablation is typically larger than that of femtosecond laser ablation because of the limited penetration length of thermal diffusion.[1,2]

Propagation velocity of the plume front in the vertical direction

The propagation velocity of the plume front in the vertical direction was evaluated by optical TOF measurements and is shown in Fig. S4. Although the variability of the velocity was largely due to the short interval (1 mm), the starting point of deacceleration was visualized.

Absorption profiles for the ambient pressure of 5.0×10^{-2} Pa

For the ambient pressure of 5.0×10^{-2} Pa, the relationships between the transmittance and the vertical position for 3 typical transient times are shown in Fig. S5. The Doppler splittings were observed at all positions and appeared after the plume front passed due to the contact layer and quasi-cavity formation in the plasma plume and the movement of atoms in the lateral direction as in the case of 3.0×10^{-4} Pa.

Pulse energy dependence on the lateral propagation velocity

The propagation velocity of the LPP plume in the lateral direction versus the pulse energy of nanosecond laser pulses is shown in Fig. S6. The typical fitting result is shown in Fig. S7.

Hyperfine structure of Al I 394.4006 nm line

Aluminium has a stable ^{27}Al isotope, and an resonance line (Al I 394.4006 nm) of

an Al atom has a hyperfine structure. Their frequency shifts with respect to the frequency of the transition without hyperfine interaction and the relative line intensities are listed in Table S1.[3] Four transitions were observed overlapping in high-temperature plasma plumes due to Doppler broadening. Thus, for temperature evaluations, the fitting function composed of four Gauss functions was used.

Table S1 Details of the hyperfine structure of Al I 394.4006 nm line.[3]

Transition	Frequency shifts, MHz	Relative intensity, –
$F = 2 \rightarrow F = 3$	1506	32
$F = 2 \rightarrow F = 2$	0	27
$F = 3 \rightarrow F = 3$	0	9
$F = 3 \rightarrow F = 2$	−1506	32
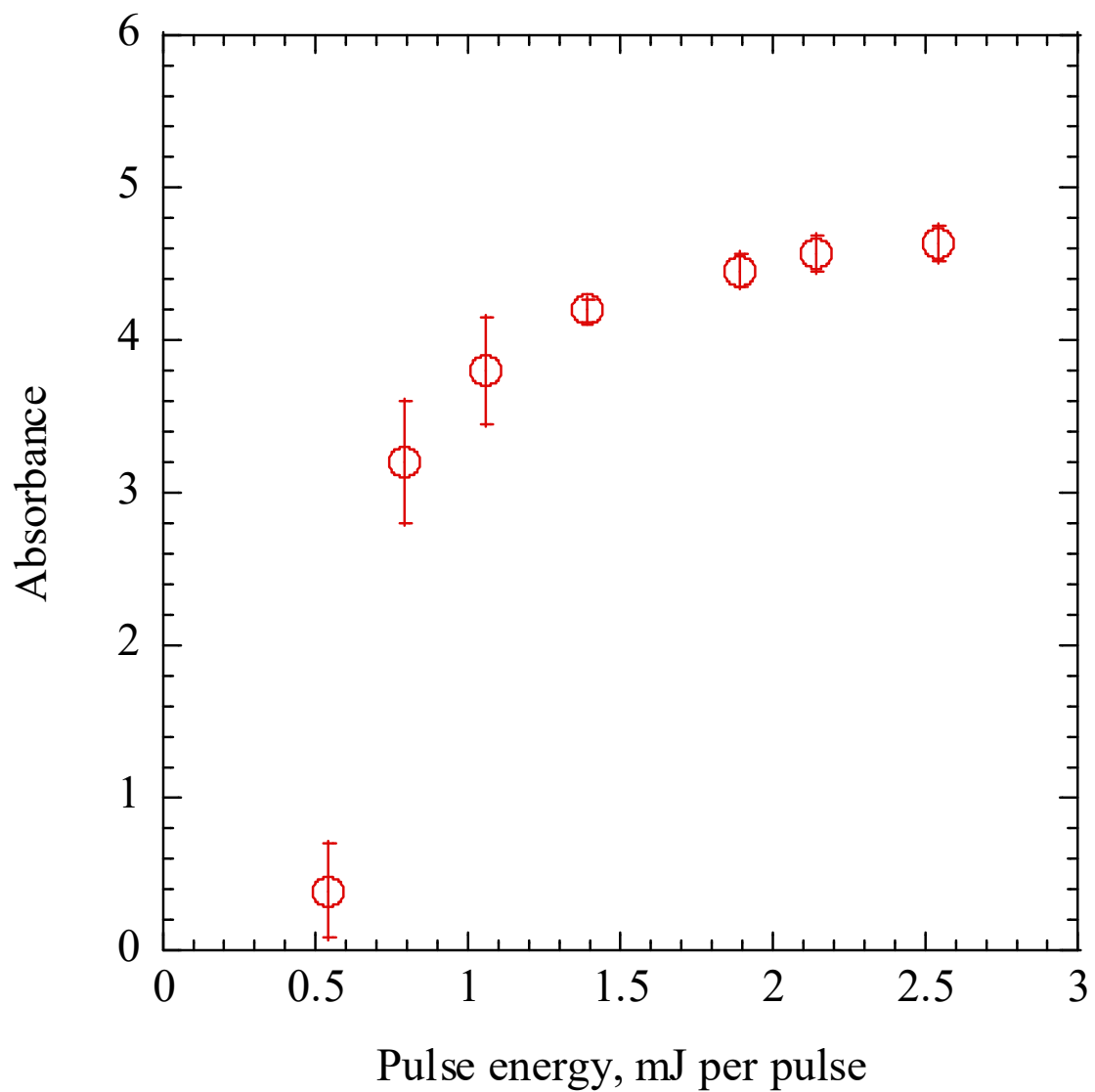
Fig. S1 Relationship between the absorbance and the pulse energy. The error bars represent the standard deviation.
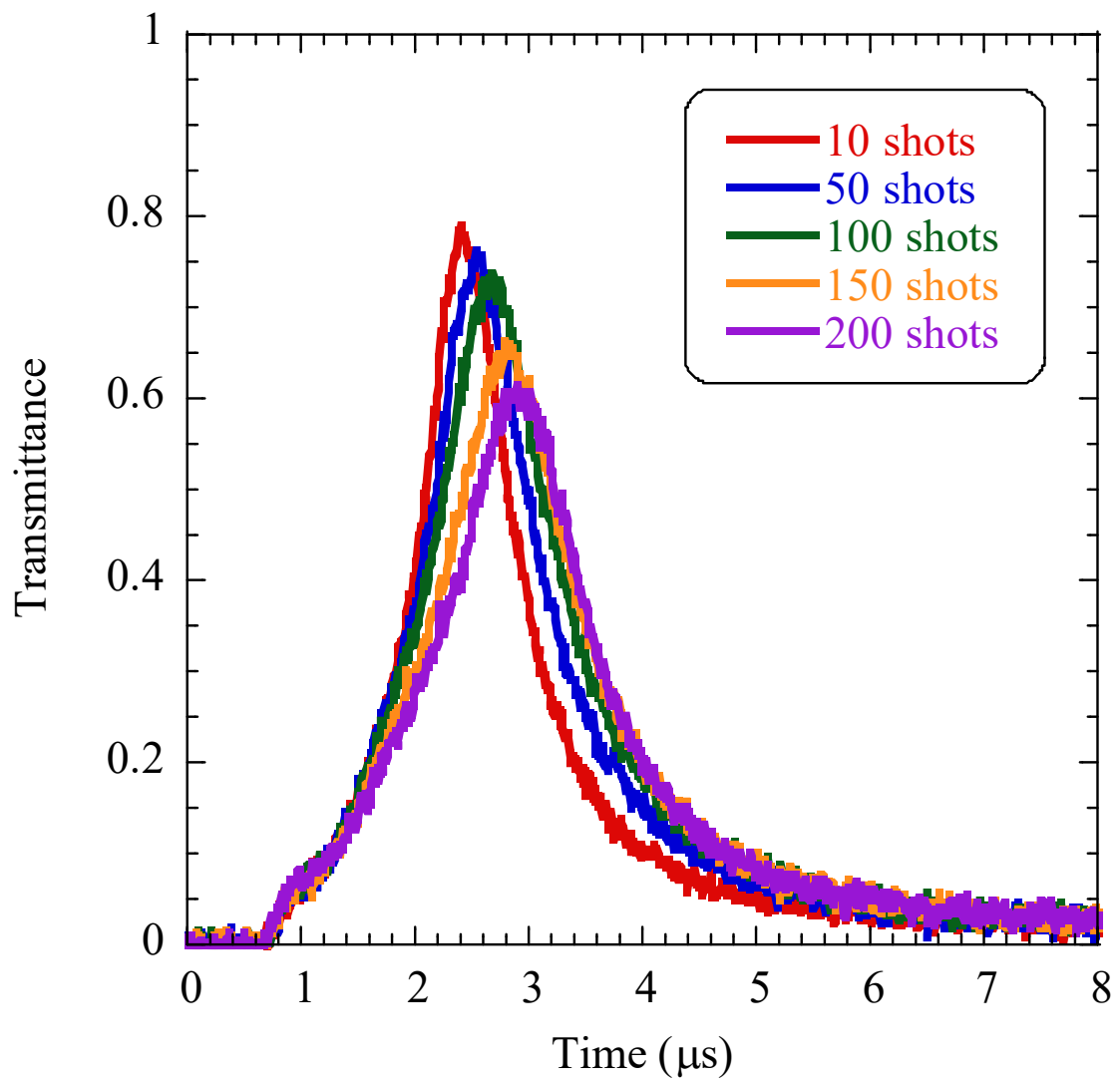
Fig. S2 Relationship between the transmittance and the number of laser shots.
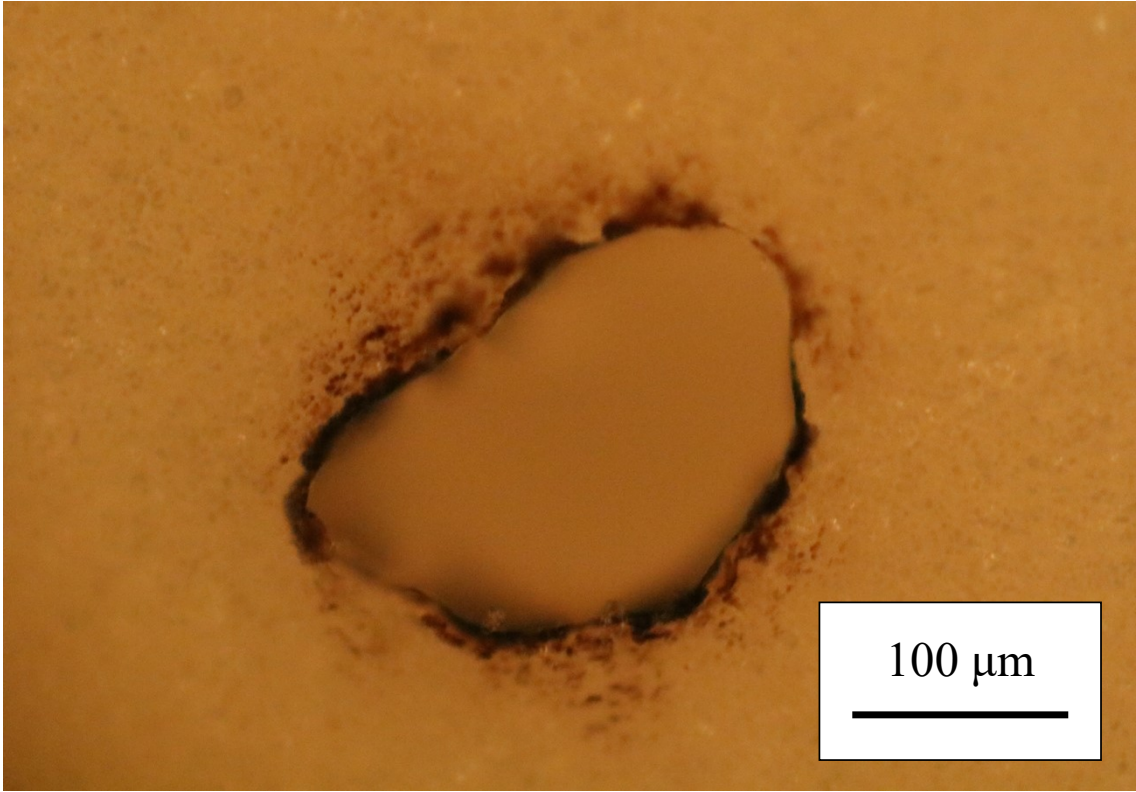
Fig. S3 Typical digital image of an ablated crater.
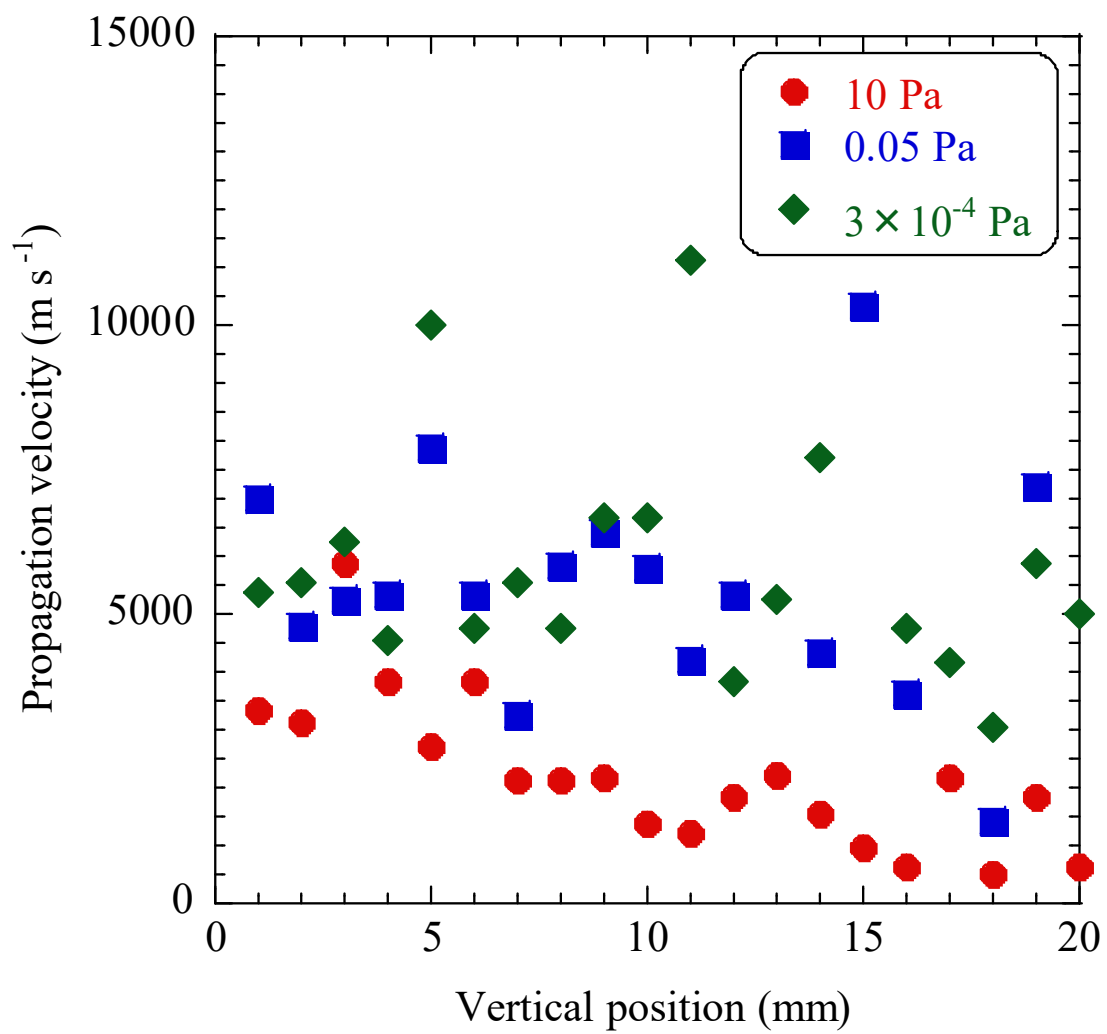
Fig. S4 Propagation velocity of the plume front in the vertical direction.

Fig. S5 Position–transmittance plots for 3 transient times and absorption spectra.
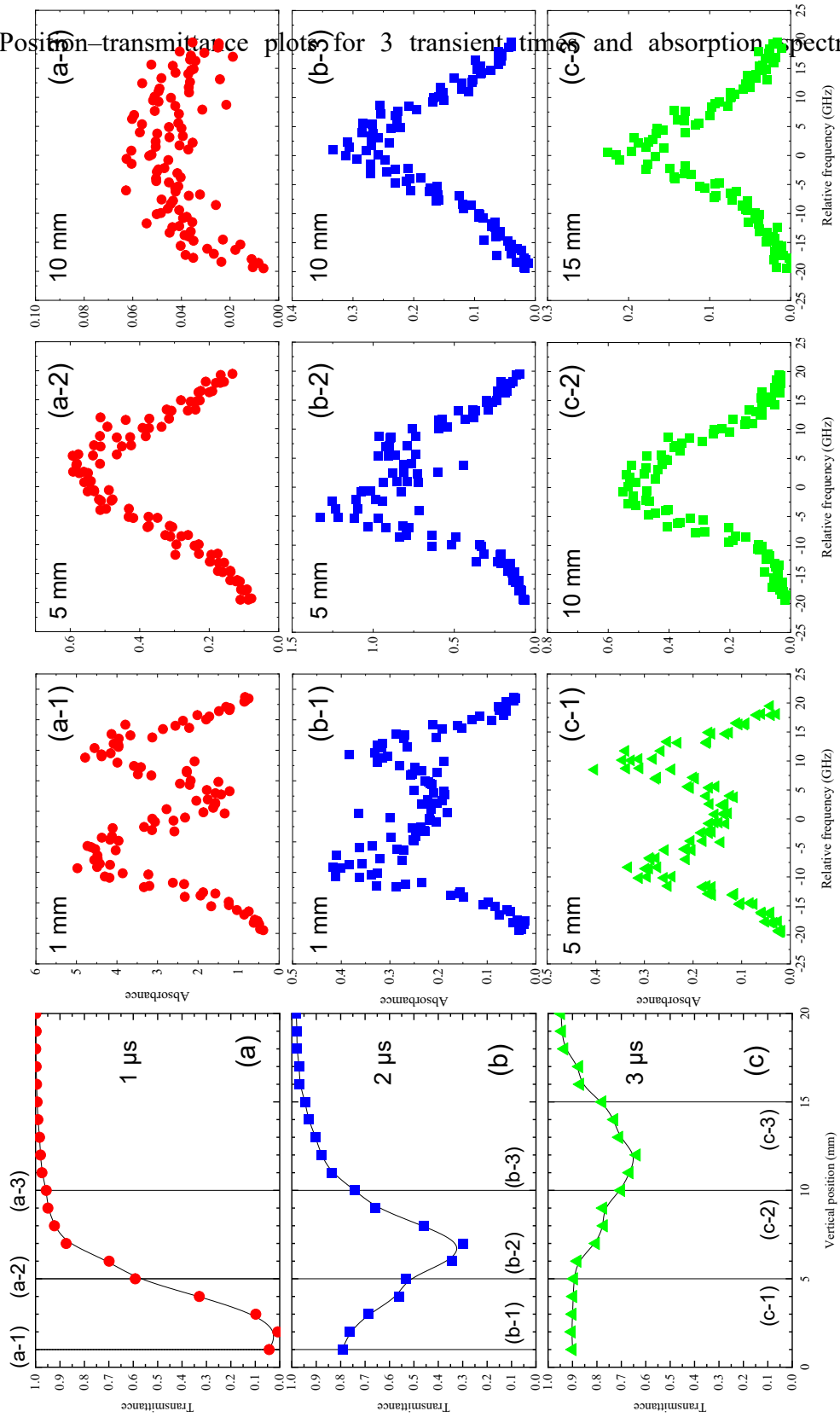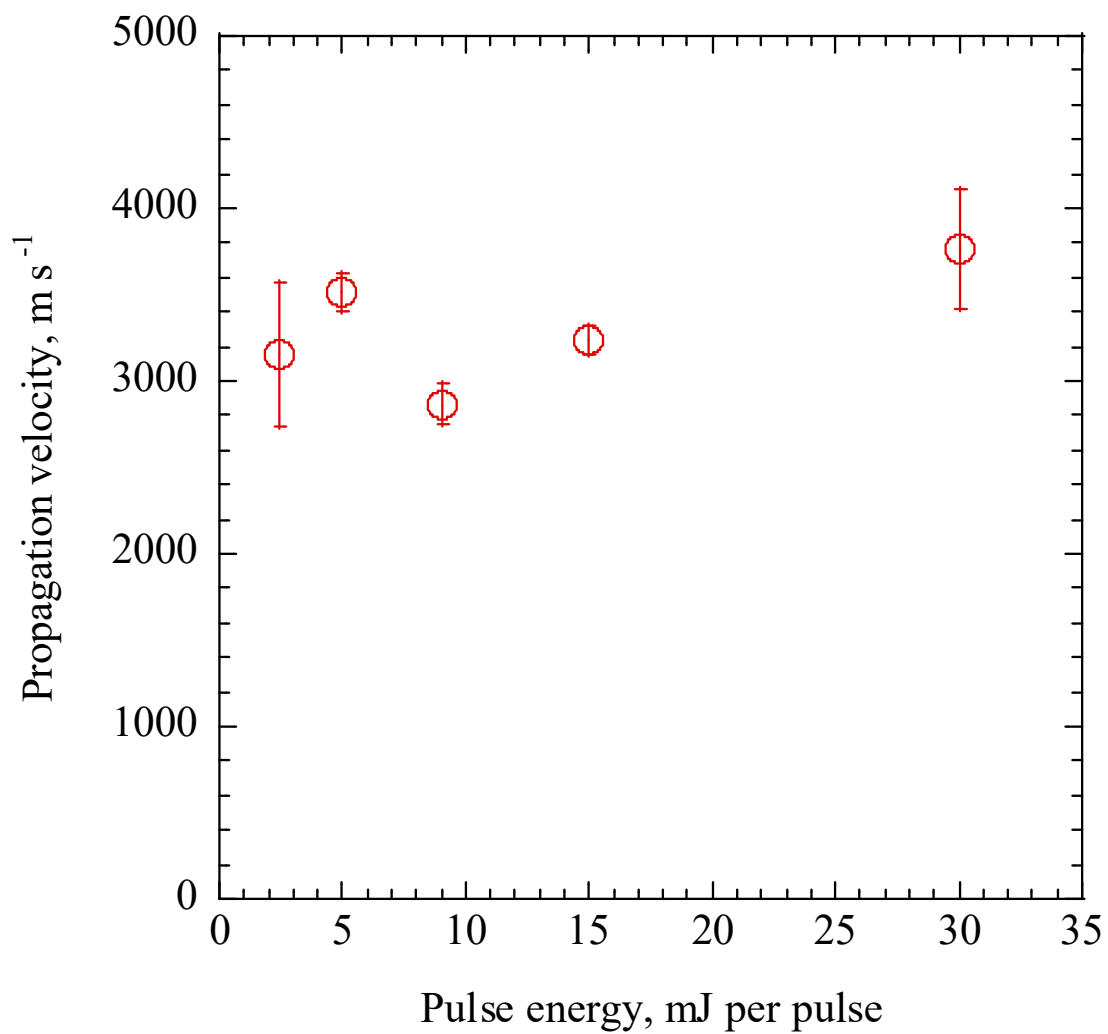
Fig. S6 Propagation velocity of the plasma plume in the lateral direction. The error bars represent the standard deviation.

$$\int k(v)\, L\, dv = S_1 + S_2$$
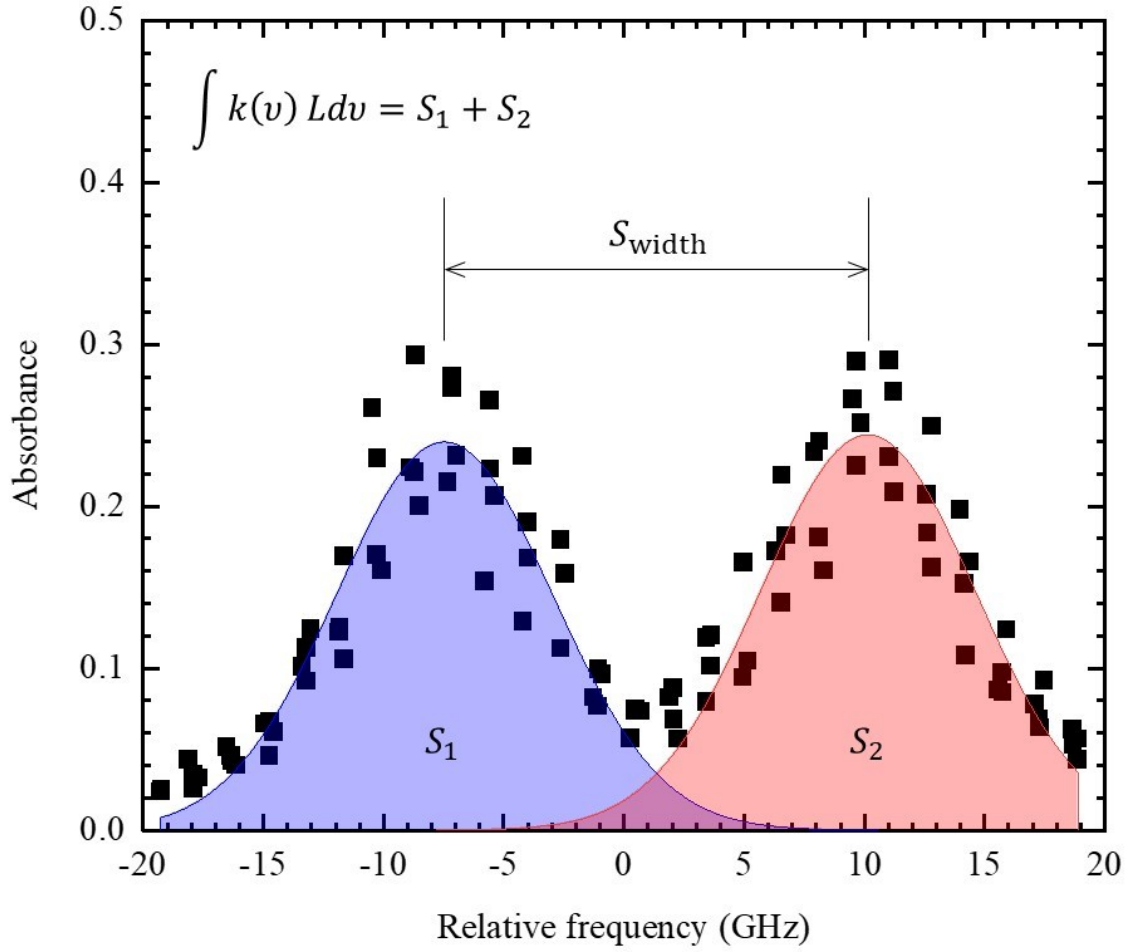
Fig. S7 Doppler components fitted to two Gaussian functions. The column number density and translational temperature were determined from the peak area and spectral width, respectively. The propagation velocity in the lateral direction was evaluated from the splitting width S_{width}.

References

1. Y. Hirayama and M. Obara, *J. Appl. Phys.*, 2005, **97**, 064903.

2. B. Verhoff, S. S. Harilal, J. R. Freeman, P. K. Diwakar and A. Hassanein, *J. Appl. Phys.*, 2012, **112**, 093303.

3. H. Scheibner, St. Franke, S. Solyman, J. F. Behnke, C. Wilke and A. Dinklage, *Rev. Sci. Instrum.*, 2002, **73**, 378.